JOURNAL OF APPLIED ELECTROCHEMISTRY **28** (1998) 545–549

Development of a novel metal hydride–air secondary battery

S. GAMBURZEV*, W. ZHANG, O. A. VELEV, S. SRINIVASAN, A. J. APPLEBY

Center for Electrochemical Systems and Hydrogen Research, Texas Engineering Experiment Station, Texas A&M University System, College Station, TX 77843-3402, USA

A. VISINTIN

Instituto Nacional de Investigaciones Fisicoquímica Teóricas y Aplicadas (INIFTA), Universidad Nacional de La Plata, Suc. 4-C.C. 16, 1900 La Plata, Argentina

Received 10 December 1996; revised 2 July 1997

A laboratory metal hydride/air cell was evaluated. Charging was via a bifunctional air gas-diffusion electrode. Mixed nickel and cobalt oxides, supported on carbon black and activated carbon, were used as catalysts in this electrode. At 30 mA cm^{-2} in 6 M KOH, the air electrode potentials were −0.2 V (oxygen reduction) and +0.65 V (oxygen evolution) vs Hg/HgO. The laboratory cell was cycled for 50 cycles at the $C/2$ rate (10 mA cm^{-2}). The average discharge/charge voltages of the cell were 0.65 and 1.6 V, respectively. The initial capacity of the metal hydride electrode decreased by about 15% after 50 cycles.

Keywords: *metal hydride/air cell*, *gas diffusion electrode*, *nickel and cobalt oxides*

1. Introduction

Nickel/metal hydride batteries are replacing nickel/cadmium batteries for certain applications because of their higher energy density, lack of a memory effect, and their low-toxicity active materials. Since 1990, many modified AB_5 and AB_2 alloys for metal hydride electrodes have been prepared and evaluated at the Center for Electrochemical Systems and Hydrogen Research in collaboration with the Brookhaven National Laboratory, the Los Alamos National Laboratory and the Hughes Aircraft Company. Some of these have shown promise for further development [1–3].

Traditional aqueous electrochemical secondary cells (e.g., Pb/PbO_2, Fe/NiOOH) have energy densities less than 50 Wh kg^{-1}, which are marginal for many new applications [4]. Both ambient-temperature secondary lithium and lithium ion cells and high-temperature alkali-metal cells (Na/S, Li/FeS) have energy densities in the 100 Wh kg^{-1} range. One category of aqueous secondary cells with energy densities in this range are metal–air systems (e.g., Zn/air, Fe/air), which eliminate the containment of the positive active material (oxygen) [4].

One possibility for increasing the energy density of secondary cells using metal hydride anodes, at the same time reducing cost, is by replacing the nickel oxide cathode by a light-weight air gas-diffusion electrode. In the case of successful realization, the metal hydride/air battery should always have a gravimetric energy density advantage over Ni/MH_X, despite its lower OCV and operating potential. Recent studies have shown promise for the development of MH_x/air [5, 6]. Because of the use of a carbon gas-diffusion electrode as the cathode, which is chemically unstable to oxygen evolution [7], a third inactive electrode to recharge the system is used in the above studies. These three-electrode systems do not have the advantages of light-weight and low cost air electrodes. The realization of a normal (two electrode) rechargeable MH_x/air battery is strongly dependent on the development of a bifunctional air gas-diffusion electrode with a stable and competitive performance for both oxygen reduction and oxygen evolution. This paper presents the initial results in the realization of a laboratory MH_x/air rechargeable cell with bifunctional air gas-diffusion cathodes. The cell was not optimized by weight and volume and at this time the obtained results are not comparable with specific gravimetric and volume parameters of other types of rechargeable batteries.

2. Experimental details

2.1. *Preparation of bifunctional catalysts and fabrication of electrodes*

There are several groups of materials described as bifunctional catalysts for oxygen reduction/evolution in gas-diffusion electrodes: (i) high surface area metals such as Pt, Ag and Ni [8, 9]; (ii) mixed metal oxides

* Visiting from Central Laboratory for Electrochemical Power Sources, 1113 Sofia, Bulgaria.

with a specific crystal structure of spinel [10], perovskite [11], or pyrochlore [12]; and (iii) some metal nitrides, sulfides or carbides [13]. A good literature review of these catalysts is described in [11]. Our earlier results in this area led to the choice of mixed nickel and cobalt oxides, supported on carbon [14], as a bifunctional catalyst in air gas-diffusion cathode. The catalysts were prepared by impregnation of powdered carbon materials with an aqueous solution of $Ni(NO_3)_2.6H_2O$ and $Co(NO_3)_2.6H_2O$ (1:2 parts by weight), followed by evaporation, drying at 100 °C, and thermal decomposition of metal nitrates on carbon at 300 °C in an air atmosphere [15]. Two types of dispersed carbon materials were used as a catalyst support: the carbon black Vulcan XC-72 (Cabot Inc.) and the activated carbon Norit SA-3 (NV Norit, The Netherlands, purchased from Aldrich). The characteristics of the as-received carbons and the compositions of the catalysts fabricated (types A and B) are given in Table 1. Figure 1 shows X-ray diffractograms of the bifunctional catalysts. Both consist of mixed NiO and CoO phases whose lattice constants are practically equal to the standard values given in the caption of Fig. 1. The significant difference between both catalysts is that in the type A catalyst supported on Norit SA-3 activated carbon, a very intense graphite peak is observed. This result is due to the fact that active carbon Norit SA-3 is initially higher graphitized than carbon black Vulcan XC-72. During the thermal decomposition of metal nitrates, the amount of graphite phase in the activated carbon Norit SA-3 relatively rises because of the intensive oxidation (burning) of the less stable amorphous part of carbon support. From these catalysts were prepared bifunctional air electrodes consisting of two PTFE-bonded (diffusion and active) layers hot pressed onto nickel mesh [16]. The total catalyst loading (carbon and metal oxides) of the bifunctional electrodes was 0.014 g cm^{-2} [14].

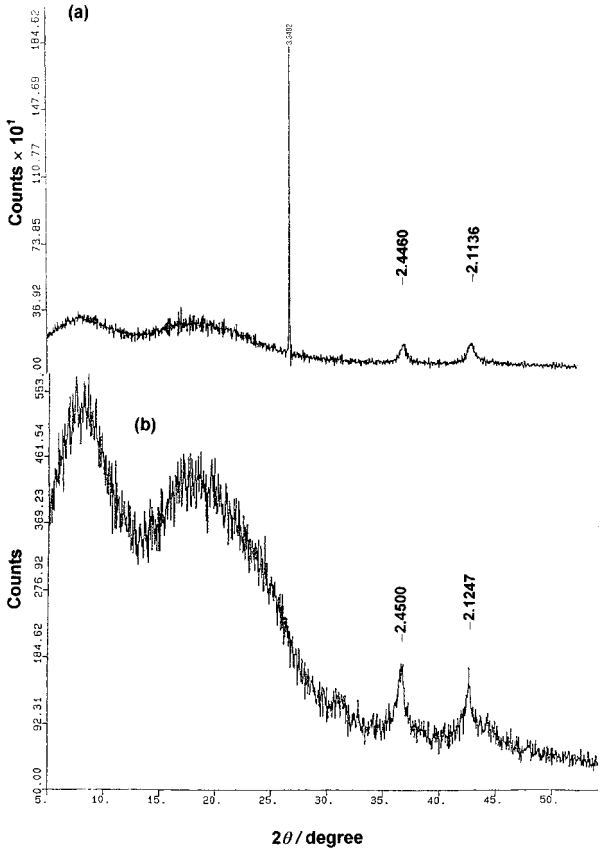

Fig. 1. X-ray diffractograms of used bifunctional catalysts: (a) catalyst type A (activated carbon Norit SA-3 with 13% NiO·CoO); (b) catalyst type B (carbon black Vulcan XC-72 with 20% NiO·CoO). Lattice constants (nm) for (i) graphite: 0.3348, –; (ii) NiO: 0.22412, 0.2088; (iii) CoO: 0.2460, 0.2130.

2.2. *Preparation of metal hydride electrodes*

The metal hydrides were of AB_5 type, with the composition $La_{0.8}Ce_{0.2}Ni_{4.25}Co_{0.5}Sn_{0.25}$. The intermetallics were prepared by helium arc-melting of the constituent elements, followed by annealing in vacuum at the desired temperatures. The intermetallics were pulverized mechanically into powders of about 325 mesh. Structure and phase density of the intermetallic samples were characterized by X-ray diffraction. Gas phase hydrogen absorption and desorption measurements were carried out in a modified Sievert's apparatus. Pressure-composition isotherms were obtained at room temperature to determine the plateau pressures and estimate the maximum equilibrium hydrogen storage capacities. Table 2 shows these characteristics in comparison with those of $LaNi_5$.

Electrodes were prepared by mechanically pressing at 3000 psi 0.075 g cm^{-2} of AB_5 alloy powder mixed with 0.075 g of Teflonized (30% PTFE) carbon black. The alloy $La_{0.8}Ce_{0.2}Ni_{4.25}Co_{0.5}Sn_{0.25}$ was used as the anode material in all experiments.

2.3. *Electrochemical measurements*

Electrochemical measurements were performed in 31 wt% KOH electrolyte, prepared from reagent grade KOH and deionized water. Electrodes were tested for their charge/discharge characteristics, initial capacity, and rate capability in a flooded electrolyte condition in open cells. Potentials were monitored using the Hg/HgO reference electrode and capacities were measured to a cut-off potential of

Table 1. Composition of bifunctional catalysts

Catalyst type	*Carbon support*	*BET surface* /m^2 g^{-1}	*Met. oxides* /wt %
A	NORIT SA-3	600	13.0
B	Vulcan XC72	250	20.0

Table 2. Physico-chemical properties of the intermetallic alloys

Alloy	*Lattice parameters*		*Maximum hydrogen*
	a/nm	*c*/nm	/Formula unit
$LaNi_5$	0.5018	0.3987	6.9
$La_{0.8}Ce_{0.2}Ni_{4.25}Co_{0.5}Sn_{0.25}$	0.50415	0.40381	5.61

−0.7 V vs Hg/HgO. The measurements were carried out using a Bitrode Battery Cycler by charging at $C/2$ rate for 2.5 to 3 h and discharging at the same rate to a cut-off cell potential of 1.0 V. The above procedure included several charge/discharge cycles to introduce metal hydride electrodes in stable work conditions.

The electrochemical measurements included polarization curves of the bifunctional electrodes operating as cathodes (oxygen reduction) and anodes (oxygen evolution) and cycle tests of the MH_x/air system. Polarization curves were obtained in a half-cell with a Hg/HgO as a reference electrode and nickel mesh as a counter electrode, whereas MH_x/air testing was conducted in a laboratory cell with an active area of 1 cm^2. All the measurements were carried out at room temperature in 31% KOH. The cells were tested at charge/discharge current densities of 0.01 A cm^{-2} ($C/2$ rate) at cut-off cell voltages of 0.6 V (discharge) and 1.65 V (charge).

3. Results and discussion

3.1. *Electrochemical characteristics of the metal hydride electrodes*

The electrochemical performance characteristics of the hydride electrodes, including discharge rate capability and cycle-life behaviour, are shown in Figs 2 and 3. Figure 2 shows the variation of discharge capacity of the alloy electrodes on prolonged cycling at the $C/2$ rate. The material used had high initial discharge capacity, which was retained at even higher initial discharge rate capabilities (Fig. 3).

3.2. *Polarization behaviour of the bifunctional electrodes*

The initial polarization curves of bifunctional electrodes which operated as oxygen reduction cathodes

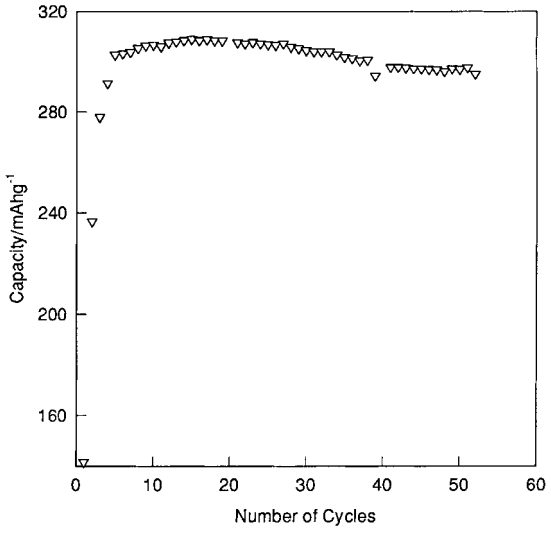

Fig. 2. Cycle life behaviour of a hydride electrode containing $La_{0.8}Ce_{0.2}Ni_{4.25}Co_{0.5}Sn_{0.25}$ alloy at $C/2$ charge and discharge, KOH 31%, $T = 25$ °C.

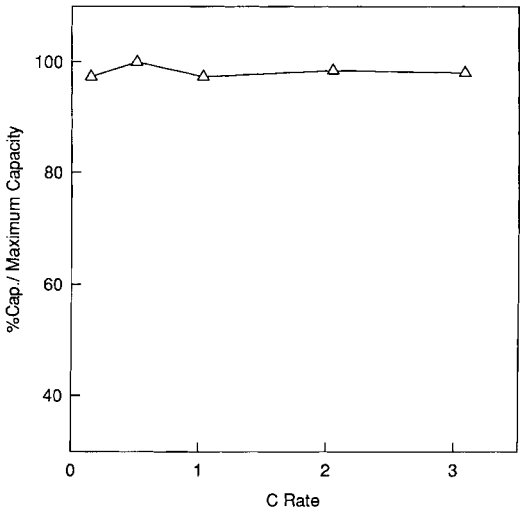

Fig. 3. Rate capabilities of a hydride electrode containing $La_{0.8}Ce_{0.2}Ni_{4.25}Co_{0.5}Sn_{0.25}$, KOH 31%, $T = 25$ °C (referenced to $C/2$ rate).

are presented in Fig. 4. The electrodes used catalyst types A, supported on activated carbon Norit SA-3, and B, supported on carbon black Vulcan XC-72 (see Table 1). These polarization curves were recorded after 24 h of electrode operation in an oxygen evolution mode at 0.01 A cm^{-2}. In earlier experiments [8], it was found that this procedure resulted in stabilization of the electrode performance. The results show that the electrode with the type A catalyst appeared to have better performance than the type B electrodes. The latter electrodes had a higher ohmic resistance, which was indicated by the higher slope of their polarization curves. This probably results from the smaller volume of pores soaked with electrolyte in type B catalysts, giving an increase in ionic resistance in the catalytic layer. This hypothesis is indirectly confirmed by the lower initial surface area of Vulcan XC 72 and the larger amount of low porous metal oxides in type B catalyst (Table 1).

Figure 5 shows the polarization curves of the same electrodes operating as oxygen evolution anodes. The polarization behaviour of type A catalyst electrodes was superior up to a current density of 0.06 A cm^{-2}, but the slope of the polarization curves was higher than that of the type B electrodes. The higher slope of

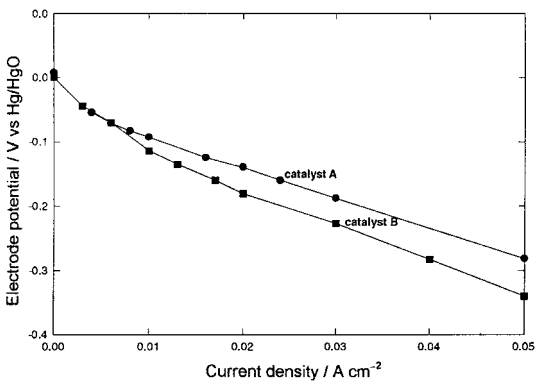

Fig. 4. Polarization curves of oxygen electrodes operated as oxygen reduction electrodes.

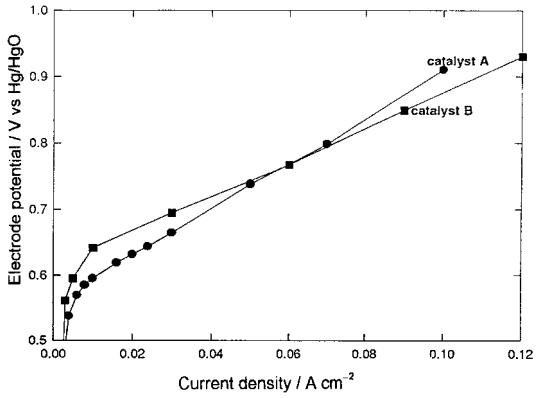

Fig. 5. Polarization curves of oxygen electrodes operated as oxygen evolution electrodes.

the polarization curve of electrodes with type A catalyst could be explained by the different sizes of pores which take place in oxygen reduction and evolution. Fine pores (or micropores [17]) cannot evolve oxygen because of the capillary overpressure. However, coarse pores (or meso- and macropores [17]) will. In contrast, neither fine nor coarse pores will work for oxygen reduction, the only active area is the three-phase boundary. Therefore, the type A catalyst must empty its coarse pores more readily than type B on oxygen evolution, giving a higher ionic resistance. Following these polarization measurements, cycling tests of laboratory MH_x/air cells were carried out using air electrodes prepared from the type A catalyst.

3.3. *Cycling tests of a laboratory metal hydride-air cell*

Cell potential against time plots for a laboratory cell at the $C/2$ rate (0.01 A cm^{-2}) during two charge/discharge cycles are shown in Fig. 6. The average charge and discharge voltages resulting from the high oxygen evolution and reduction overpotentials were 1.60 and 0.65 V, respectively. The energy efficiency of the system calculated from these values was about 40%. However, the cell design had a 4 cm gap between the metal hydride and oxygen electrodes to minimize the

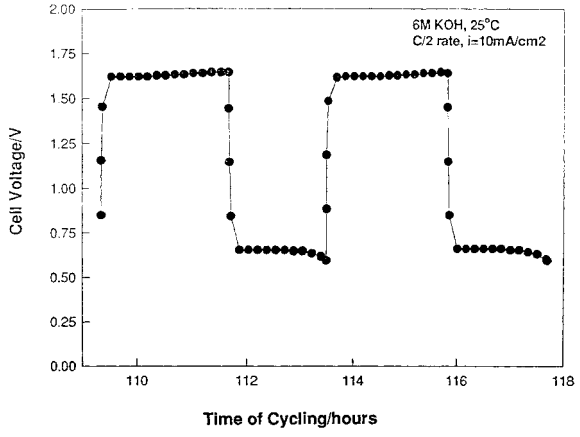

Fig. 6. Charge/discharge behaviour of the metal hydride/air cell during 25 and 26 cycles. Conditions: 6 M KOH, 25 °C, $C/2$ rate, $i = 10\,\text{mA cm}^{-2}$.

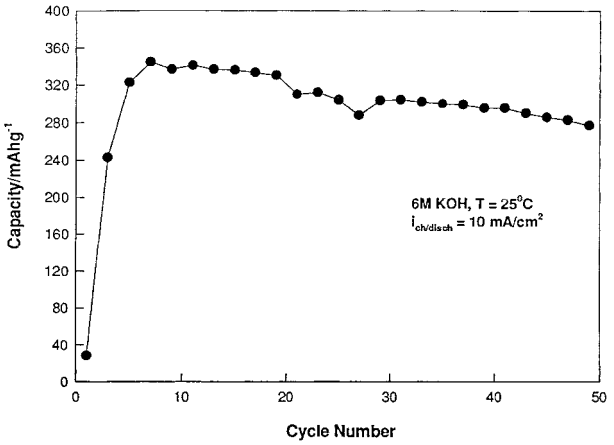

Fig. 7. Plot of capacity of the metal hydride/air cell as a function of number of cycles. Conditions: 6 M KOH, $T = 25\,^{\circ}\text{C}$, $i_{\text{ch/disch}\cdot} = 10\,\text{mA cm}^{-2}$.

negative influence of hydroperoxide anion HO_2^- generated at the oxygen electrode during discharge on the metal hydride anode. Obviously, it was not optimized for cell operation and estimation of energy efficiency. The cell maintained a stable potential during charge and discharge. A plot of the specific capacity of the cell (determined by the capacity of the metal hydride electrode only) as a function of the number of cycles is presented in Fig. 7. It has been generally observed that freshly prepared alloy electrodes do not absorb hydrogen to their optimum capacity until after several cycles. The 'activation' of the alloy due to removal of the surface oxides would lead to an increase in the active surface area, and thus, enhance the hydrogen absorption. The number of cycles to activate the alloy electrodes and to attain full capacity depends on the type of the alloy. After 50 cycles, the capacity of the system had decreased by 15%. It could be assumed that the capacity loss was due to partial surface oxidation of the metal hydride by reaction with dissolved oxygen or hydroperoxide anions HO_2^- diffusing from the cathode during discharge, in spite of a big distance (4 cm gap) between the electrode in the test cell. The deterioration of oxygen electrode performance is illustrated by Figs 8 and 9. There was no apparent decrease in the elec-

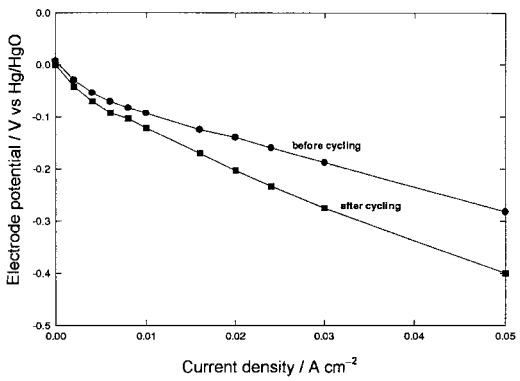

Fig. 8. Polarization curves of the oxygen electrode operating in the oxygen reduction mode before and after cycling.

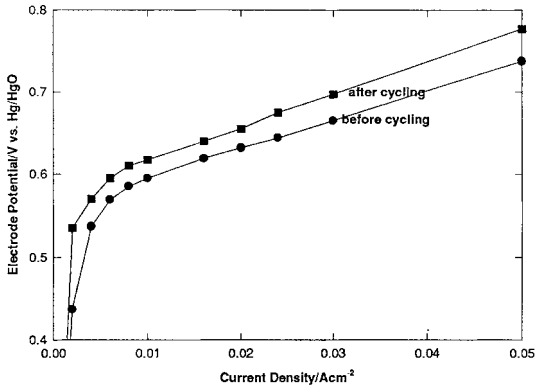

Fig. 9. Polarization curves of the oxygen electrode operating in the oxygen evolution mode before and after cycling.

trocatalytic activity of the electrode operating in the discharge mode, but an increase of its ohmic resistance was observed (Fig. 8). In the charge mode, some decrease in electrocatalytic activity combined with a slight increase in ohmic resistance was observed (Fig. 9). Generally, at least two processes could negatively influence the performance of the air gas diffusion electrode during its long time operation as an oxygen reduction electrode: (i) oxidation of the carbon surface due to the decomposition of hydroperoxide anion HO_2^- which is an intermediate product of oxygen reduction; and (ii) formation of potassium carbonates due to the reaction between alkaline electrolyte (KOH) and CO_2 in atmospheric air (carbonization of the electrolyte). In our earlier publication [18], it was shown experimentally that the first of the above processes predominates in the electrode performance failure during long time operation. Additionally, some chemical and mechanical degradation of the electrode structure takes place during oxygen evolution. Further work to solve these problems are in progress.

4. Conclusions

(i) The results obtained show that it is possible to operate a metal hydride/air secondary battery as an alternative to the nickel/metal hydride or the metal/air systems.

(ii) Previous work showed that uncatalyzed carbons (including Norit and Vulcan types) were rapidly oxidized during oxygen evolution [9]. The negative effect can be significantly reduced by the presence of mixed Co–Ni oxides as catalysts, which appear to protect the carbon support, which may result from the thermal treatment step to decompose the mixed nickel/cobalt oxide catalysts.

(iii) The energy efficiency of the laboratory system described is currently only 40%. This value can be increased by minimizing the internal resistance of the cell and with an improvement of the bifunctional air electrode.

(iv) To achieve an acceptable cycle life of the system, the metal hydride anode must be protected from surface oxidation, which requires further development of a suitable method of protection of the metal hydride electrode.

Acknowledgements

The authors acknowledge the sponsorship of this work by the Chemical Science Division, Office of Basic Energy Sciences, US Department of Energy (Contract No. DE-FG03-93ER14381), and the Texas Higher Education Coordinating Board (Grant 717500).

References

[1] A. Anani, A. Visintin, K. Petrov, S. Srinivasan, J. J. Reilly, J. R. Johnson, R. Schwarz and P. Desch, *J. Power Sources* **47** (1994) 261.
[2] P. Folonary, G. Iemmi, F. Manfredi and A. Rolle, *J. Less-Comm. Met.* **74** (1980) 371.
[3] K. Videm, *in* 'Hydrides for Energy Storage' (edited by A. F. Andersen and A. E. Maeland), Pergamon Press (1978).
[4] D. Linden (Ed.), 'Handbook of batteries', McGraw-Hill, New York (1996), p. 35.11
[5] H. Sakai, T. Iwaki, Z. Ye, D. Noreus and O. Lindstrom, 186th ECS Meeting, Miami FL, 9–14 Oct., 1994, Extended Abstracts, Abstr. 68, p. 108.
[6] H. Sakai, T. Iwaki, Z. Ye, D. Noreus and O. Lindstrom, *J. Electrochem. Soc.* **142** (1995) 4040.
[7] A. J. Appleby, G. Crepy and G. Feuillate, *Power Sources 6* (edited by D. H. Collins), Academic Press, London (1977), p. 549.
[8] O. C. Wagner, *J. Electrochem. Soc.* **116** (1969) 693.
[9] L. Carlsson and L. Ojefors, *ibid.* **127** (1980) 525.
[10] A. C. C. Tseung and K. L. K. Yeung, *ibid.* **125** (1978) 1003.
[11] Y. Shimizu, K. Uemura, H. Matsuda, N. Miura and N. Yamazoe, *ibid.* **137** (1990) 3430.
[12] H. S. Horovitz, J. M. Longo and H. H. Horovitz, *ibid.* **130** (1983) 1851.
[13] E. S. Buzzelli, C. T. Liu and W. A. Briant, 'Proc. of the 12th IECEC', San Diego, CA (1978), p. 745.
[14] S. Gamburzev, unpublished results (1980).
[15] S. Gamburzev, A. Kaisheva, P. Atanassov and I. Iliev, *Bulgarian Patent 93611* (10 Jan. 1991).
[16] I. Iliev, S. Gamburzev, A. Kaisheva and J. Mrha, *J. Appl. Electrochem.* **5** (1975) 291.
[17] M. M. Dubinin, *in* 'Metodi issledovaniya katalizatorov i kataliticeckih reakcij', Nauka, Novosibirsk, No. 4 (1971), pp. 37–55.
[18] S. Gamburzev, *Elektrokhimya* **18** (1982) 134.